Clinical Immunology 251 (2023) 109628

Contents lists available at ScienceDirect

Clinical Immunology

journal homepage: www.elsevier.com/locate/yclim

Triple immune modulator therapy for aberrant hyperinflammatory responses in severe COVID-19

June-Young Koh [a,1], Jae-Hoon Ko [b,1], So Yun Lim [c,1], Seongman Bae [c], Kyungmin Huh [b], Sun Young Cho [b], Cheol-In Kang [b], Doo Ryeon Chung [b], Chi Ryang Chung [d], Sung-Han Kim [c,*,2], Kyong Ran Peck [b,**,2], Jeong Seok Lee [a,e,***,2]

[a] Genome Insight, Inc., San Diego, La Jolla, CA, USA
[b] Division of Infectious Diseases, Department of Medicine, Samsung Medical Center, Sungkyunkwan University School of Medicine, Seoul, Republic of Korea
[c] Department of Infectious Diseases, Asan Medical Center, University of Ulsan College of Medicine, Seoul, Republic of Korea
[d] Department of Critical Care Medicine, Samsung Medical Center, Sungkyunkwan University School of Medicine, Seoul, Republic of Korea
[e] Graduate School of Medical Science and Engineering, Korea Advanced Institute of Science and Technology (KAIST), Daejeon, Republic of Korea

ARTICLE INFO

Keywords:
Glucocorticoid
Tocilizumab
Baricitinib
Severe
COVID-19

ABSTRACT

A dysregulated hyperinflammatory response is a key pathogenesis of severe COVID-19, but optimal immune modulator treatment has not been established. To evaluate the clinical effectiveness of double (glucocorticoids and tocilizumab) and triple (plus baricitinib) immune modulator therapy for severe COVID-19, a retrospective cohort study was conducted. For the immunologic investigation, a single-cell RNA sequencing analysis was performed in serially collected PBMCs and neutrophil specimens. Triple immune modulator therapy was a significant factor in a multivariable analysis for 30-day recovery. In the scRNA-seq analysis, type I and II IFN response-related pathways were suppressed by GC, and the IL-6-associated signature was additionally downregulated by TOC. Adding BAR to GC and TOC distinctly downregulated the ISGF3 cluster. Adding BAR also regulated the pathologically activated monocyte and neutrophil subpopulation induced by aberrant IFN signals. Triple immune modulator therapy in severe COVID-19 improved 30-day recovery through additional regulation of the aberrant hyperinflammatory immune response.

1. Introduction

Numerous immune modulators have been developed to treat chronic inflammatory diseases (1–4). Since the first approval of tumor necrosis factor-α (TNF-α)-blocking agents for rheumatoid arthritis, targeted immune modulators have revolutionized the treatment of inflammatory arthritis, including interleukin-6 (IL-6) inhibitors and Janus kinase (JAK) inhibitors (1–4). IL-6 inhibitors control macrophage activation syndrome and cytokine release syndrome (5–7), and glucocorticoids (GCs), the prototype of immune modulators, have been used to control hyperinflammation caused by infectious diseases (8,9). Coronavirus disease 2019 (COVID-19) is the first viral infection for which immunosuppressive agents play a major role in treatment and the pathogenesis of the illness is under investigation (10–15).

Dysregulated hyperinflammation after severe acute respiratory syndrome coronavirus 2 (SARS-CoV-2) infection is a key pathogenetic mechanism of the tissue damage seen with severe COVID-19 (16–18). Current guidelines recommend administration of immune modulators, particularly GCs, IL-6 inhibitors (tocilizumab (TOC) or sarilumab), or JAK inhibitors (baricitinib (BAR) or tofacitinib) to treat severe COVID-

* Correspondence to: Sung-Han Kim, Department of Infectious Diseases, Asan Medical Center, University of Ulsan College of Medicine, 88, Olympic-ro 43-gil, Songpa-gu, Seoul 05505, Republic of Korea.
** Correspondence to: Kyong Ran Peck, Division of Infectious Diseases, Department of Medicine, Samsung Medical Center, Sungkyunkwan University School of Medicine, 81 Irwon-ro, Gangnam-gu, Seoul 06351, Republic of Korea.
*** Correspondence to: Jeong Seok Lee, Graduate School of Medical Science and Engineering, Korea Advanced Institute of Science and Technology (KAIST), 291 Daehak-ro, Yuseong-gu, Daejeon 34141, Republic of Korea.
E-mail addresses: kimsunghanmd@hotmail.com (S.-H. Kim), krpeck@skku.edu (K.R. Peck), chemami@kaist.ac.kr (J.S. Lee).
[1] These first authors contributed equally to this article.
[2] These corresponding authors contributed equally to this article.

https://doi.org/10.1016/j.clim.2023.109628
Received 20 January 2023; Accepted 26 April 2023
Available online 27 April 2023

19 (10–15). The clinical recovery or survival benefits of these agents have been demonstrated through phase 3 randomized controlled trials (RCTs), but the 28-day mortality rate of severe COVID-19 was still high, 20–30%, even in the treatment arms (11–13). Clinicians have tried various combinations or dose adjustments of immune modulators when treating severe COVID-19 (19–24). Although current guidelines do not support combined use of TOC and BAR because of a potential additive risk of infection (10,15), robust clinical or experimental data that support or oppose combined use of immune modulators for severe COVID-19 are scarce. Therefore, we conducted a retrospective cohort study comparing Single (GC only), Double (GC and TOC) and Triple (GC, TOC, and BAR) immune modulator therapy for severe COVID-19 during a delta-dominated outbreak period. To immunologically investigate the effects of the immune modulator therapies, a single-cell RNA sequencing (scRNA-seq) analysis was performed in serially collected peripheral blood mononuclear cells (PBMCs) and neutrophil specimens.

2. Methods

2.1. Study design and population

A retrospective cohort study was conducted at two tertiary care hospitals designated for severe COVID-19 patient care between July 2021 and October 2021, the delta-dominated, 4th national outbreak period in Republic of Korea (25). The hospitals are 5 km apart and share a local COVID-19 outbreak situation. Severe COVID-19 patients requiring an O_2 supply >5 L per min via facial mask were referred or admitted directly to the intensive care units (ICUs) of these centers. The diagnosis of COVID-19 was based on real-time polymerase chain reaction (RT-PCR) tests for SARS-CoV-2 using test kits approved by the Korean Ministry of Food and Drug Safety under an emergency use authorization (26). Patients with severe COVID-19 who required O_2 support via a high flow nasal cannula (HFNC) or non-invasive ventilation (WHO-Clinical Progression Scale 6) and received TOC treatment in addition to a GC (mostly dexamethasone) were screened for this study (27). Patients who were intubated before or on the day of admission and those with do-not-resuscitate status were excluded from these analyses.

During the study period, Hospital A (double immune modulator group) implemented a guideline-based treatment protocol of dexamethasone (6 mg iv q24hr for up to 10 days) and a single dose of TOC (8 mg/kg at admission), in addition to remdesivir for 5 days, low molecular-weight heparin (LMWH) for deep vein thrombosis (DVT) prophylaxis, antacid for peptic ulcer prophylaxis, and trimethoprim/sulfamethoxazole (TMP/SMX) for *Pneumocystis jirovecii* pneumonia (PJP) prophylaxis. Hospital B (triple immune modulator group) implemented an aggressive severity-adjusted treatment protocol, based on guidelines, published studies, and clinical experiences (10,15,23,24,26,28). The therapy consisted of dose-adjusted dexamethasone (ranging from 0.1 mg/kg to 0.2 mg/kg iv q24hr), TOC (8 mg/kg up to 2nd dose), and BAR (up to double dose), in addition to remdesivir for up to 10 days, LMWH for DVT prophylaxis, antacid for peptic ulcer prophylaxis, TMP/SMX for PJP prophylaxis, and itraconazole for COVID-19-associated pulmonary aspergillosis (CAPA) prophylaxis. The detailed institutional treatment protocols of each hospital are illustrated in Supplementary Fig. 1. This retrospective cohort study was approved by the institutional review boards (IRB) of each hospital (IRB no. AMC 2020–0297, AMC 2020–0299, and SMC 2021–09-080), and the requirement for informed consent was waived because de-identified retrospective data were used for analysis.

To immunologically investigate the effects of the immune modulator therapies, serial blood specimens were collected from patients with severe COVID-19 who were admitted to Hospital B between August 2020 and November 2021. During that period, patients were treated with GC alone (single immune modulator), double immune modulators, or triple immune modulators, in serial order (24). PMBCs were collected from all three immune modulator groups, but neutrophils were separated only from the triple immune modulator group. Secreted cytokines were measured in serum specimens of non-overlapping severe COVID-19 patients who were treated with single, double, and triple immune modulators between February 2020 and April 2022. This immunologic investigation was conducted among patients who agreed to undergo the testing and was approved by the IRB of Samsung Medical Center (IRB no. SMC 2020–03-113), with written informed consent obtained from each patient.

2.2. Data collection and outcome assessment

Baseline characteristics, treatment modalities, and outcome data were retrospectively collected from the electronic medical records. The demographic data collected were age, sex, vaccination history, and the interval between symptom onset and ICU admission. Initial status at the time of ICU admission was assessed using the initial cycle threshold (Ct) values of RT-PCR, FiO_2 at ICU admission, and peak FiO_2 within three days of admission. Initial laboratory test results and underlying diseases were also recorded. Information about treatment modalities, treatment duration, cumulative dose of dexamethasone, administration interval of tocilizumab and baricitinib, and administration of other treatment modalities was collected. The primary endpoint was clinical recovery by hospital day (HD) 30, defined as no O_2 requirement (WHO-CPS $\leq$ 4). For patients who used home O_2 at baseline, recovery to baseline O_2 was considered to be clinical recovery. Infectious complications, the slope of FiO_2 until HD 15, endotracheal intubation (WHO-CPS 7 or 8), extracorporeal membrane oxygenation (ECMO) (WHO-CPS 9), duration of hospital stay, and in-hospital death (WHO-CPS 10) were investigated as secondary outcomes.

2.3. Cell isolation

PBMCs were isolated by density gradient centrifugation using Lymphocyte Separation Medium (Corning, NY, USA). The obtained single-cell suspensions were cryopreserved in fetal bovine serum (Corning, NY, USA) containing 10% dimethyl sulfoxide (Sigma-Aldrich) until use. For neutrophil analysis, fresh peripheral blood from donors was centrifuged at 400 $\times g$ for 10 min at 4 °C. The supernatant was removed, and the cell pellet was suspended and incubated in 10 ml 1 × lysis buffer (Thermo Fisher, MA, USA), for 10 min at room temperature. After the red blood cell (RBC) lysis reaction, 20 ml of 1× phosphate-buffered saline was added to stop the lysis reaction, followed by centrifugation at 500 $\times g$ for 5 min at 4 °C. The isolated leukocytes were immediately subjected to single-cell library preparation without freezing.

2.4. scRNA-seq analysis

scRNA-seq libraries were generated using a Chromium Next GEM Single Cell 3′ GEM, Library & Gel Bead Kit v3.1 (10× Genomics, CA, USA) and following the manufacturer's instructions. Libraries were constructed and sequenced at a depth of approximately 15,000 reads per cell for gene expression using the Novaseq 6000 platform (Illumina, CA, USA). The sequenced data were de-multiplexed, aligned to the human reference genome (GRCH38; 10× Cell Ranger reference GRCh38 v3.0.0), and counted using Cell Ranger (10× Genomics). Libraries of whole leukocytes with neutrophil were overridden by the cell-calling algorithm using the 'cellranger count' function with the '–force-cells' option, to capture neutrophils with a low Unique Molecular Identifier (UMI) count. The count matrix was analyzed using the Seurat R package during the following analysis (Seurat, v4.1.0; 31,178,118). For basic quality control, we de-convoluted the sample identity and filtered inter-individual multiplets using the demuxlet package (29). We filtered low-quality cells expressing mitochondria genes >7.5% or < 0.5% of their total gene expression or with <500 or > 4500 genes. Next, standard normalization for the gene expression of each cell was performed based

on the total read count and identification of highly variable genes (n = 2000). Then, the fast mutual nearest neighbors (fastMNN) method was used to integrate and correct batch effects according to GEM origin (30). The integrated matrix was dimensionally reduced and visualized using uniform manifold approximation and projection (UMAP) with the top 20 MNN components for whole PBMCs and the top 30 MNN components for whole leukocytes for neutrophil analysis. Intra-individual multiplets were filtered out after initial unsupervised clustering. Last, the cells underwent unsupervised clustering and annotation according to marker gene expression.

The differentially expressed genes (DEGs) in each cluster relative to the other clusters were calculated on the basis of the Wilcoxon rank sum test in Seurat's implementation (FindAllMarkers function) using a > 0.25 log fold change compared with the other clusters and a Bonferroni-adjusted p-value <0.05. To describe the characteristics of each sub-cluster, we performed gene set enrichment analysis (GSEA) by calculating gene set module score (AddModuleScore in Seurat package), combined score (enrichR) (31), and enrichment score (GSEA v4.2.3, Broad Institute, CA, USA) with publicly available gene sets, including the Gene Ontology: Biological process databases (GO.BP) (32), LINCS L1000 data (33), and gene sets from severe COVID-19 patients (34). The GO.BP terms related to immune responses were filtered using the following inclusion criteria: "T_CELL", "IMMUNE", "INNATE", "ADAPTIVE", "INFLAM", "INTERLEUKIN", "INTERFERON", "NECROSIS", "APOPTOSIS", "SENESCENCE", "NATURAL", "LYMPHOCYTE", "LEUKOCYTE", "TRANSFORMING", "CHEMO", "CYTOTO", "CYTOKINE", "ANTIGEN", and "SIGNALING".

2.5. Statistical analysis

To compare clinical variables, Student's t-test or the Mann-Whitney U test was used for continuous variables, and the chi-square or Fisher's exact test was used for categorical variables. The Kaplan Meier method was used to calculate the 30-day probability of recovery, and Cox proportional hazard models were used to evaluate potential effects of each variable on clinical recovery by HD 30. All collected factors relevant to the outcomes were evaluated in univariable analyses, and statistically significant factors were included in multivariable analysis. For comparison of FiO_2 improvement between the two groups, a linear mixed model including a random effect intercept was performed to consider the variance due to repeated measurement data in the same patient. Residual plots were considered for model diagnosis. All P-values were two-tailed, and those <0.05 were considered to be statistically significant. IBM SPSS Statistics version 20.0 (IBM Corporation, Armonk, NY, USA) and R software (version 4.0.0 with packages; The R Foundation for Statistical Computing, Vienna, Austria) were used for all statistical analyses.

3. Results

3.1. Baseline characteristics of severe COVID-19 patients

During the study period, 126 patients with severe COVID-19 requiring HFNC support and TOC treatment were screened. After excluding 24 patients who were intubated before or on the day of admission, 102 patients were included in the study cohort and classified as the double immune modulator group (Double group; n = 52) or triple immune modulator group (Triple group; n = 50) (Supplementary Fig. 2). The baseline characteristics of the cohort patients are presented in Table 1. Demographics (age, sex, vaccination history, and symptom onset to ICU admission) did not differ between the two groups. At ICU admission, all patients required HFNC (WHO-CPS 6), and none of the other severity variables differed between the groups. Initial laboratory test results and underling diseases were similar between the Double and Triple groups, except albumin (2.7 ± 0.4, 3.7 ± 0.4 g/dL, respectively; P < 0.001) and C-reactive protein (CRP) (11.2 ± 8.0, 7.4 ± 6.3 mg/dL, respectively; P = 0.009) levels.

Table 1
Baseline characteristics of the cohort patients.

Variables	Double immune modulator (n = 52)	Triple immune modulator (n = 50)	P value
Demographics			
Age, years	54.7 ± 11.1	58.2 ± 12.5	0.144
Male sex	36 (69.2)	37 (74.0)	0.664
Vaccination within 2 weeks, any	10 (19.2)	10 (20.0)	1.000
Adenovirus vectored vaccine	6 (11.5)	7 (14.0)	0.773
mRNA vaccine	4 (7.7)	3 (6.0)	0.735
Interval from 1st dose to Sx onset, days	65.4 ± 38.5	81.5 ± 44.1	0.412
2nd dose finished	2 (3.8)	5 (10.0)	0.219
Sx onset to ICU admission, days	7.4 ± 3.8	7.9 ± 3.2	0.457
Initial presentation at ICU admission			
WHO-CPS 6	52 (100.0)	50 (100.0)	1.000
Initial Ct value, LRT (ORF1ab)	25.3 ± 5.9	22.7 ± 5.9	0.061
FiO_2 at ICU admission	58.0 ± 19.6	57.4 ± 17.2	0.870
Peak FiO_2 within 3 days	64.2 ± 18.1	64.8 ± 19.4	0.878
Initial laboratory tests			
WBC count, $x10^3/\mu L$	6.7 ± 3.2	7.9 ± 3.3	0.080
Lymphocyte count, $x10^3/\mu L$	0.8 ± 0.4	0.8 ± 0.4	0.972
Platelet count, $x10^3/\mu L$	229.4 ± 140.1	226.2 ± 107.3	0.897
Albumin, g/dL	2.7 ± 0.4	3.7 ± 0.4	<0.001
BUN, mg/dL	16.8 ± 9.0	17.6 ± 10.1	0.709
Creatinine, mg/dL	0.9 ± 0.4	0.8 ± 0.3	0.348
LDH, IU/L	496.4 ± 208.6	545.2 ± 156.4	0.186
CRP, mg/dL	11.2 ± 8.0	7.4 ± 6.3	0.009
Underlying diseases			
Obesity (BMI > 25 kg/m^2)	16 (30.8)	23 (46.0)	0.154
Hypertension	15 (28.8)	13 (26.0)	0.826
Diabetes mellitus	14 (26.9)	14 (28.0)	1.000
Cardiovascular disease	5 (9.6)	3 (6.0)	0.497
Pulmonary disease	1 (1.9)	5 (10.0)	0.083
Liver disease	4 (7.7)	1 (2.0)	0.183
Renal disease	0 (0.0)	1 (2.0)	0.305
Solid cancer	2 (3.8)	1 (2.0)	0.581
Hematologic malignancy	0 (0.0)	1 (2.0)	0.305
Charlson Comorbidity Index	0 (0–1)	0 (0–1)	0.969

Data are expressed as the number (%) of patients, mean ± SD, or median (IQR) values unless indicated otherwise.
Abbreviations: mRNA, messenger ribonucleic acid; Sx, symptom; ICU, intensive care unit; WHO-CPS, World Health Organization Clinical Progression Scale; Ct, cycle threshold; LRT, lower respiratory tract; ORF1ab, open reading frame 1ab; FiO_2, fraction of inspired oxygen; WBC, white blood cell; BUN, blood urea nitrogen; LDH, lactate dehydrogenase; CRP, C-reactive protein; BMI, body mass index.

3.2. Clinical outcomes of the cohort patients according to treatment strategy

The treatments and outcomes of the cohort patients are summarized in Table 2. According to the severity-adjusted treatment protocol of Hospital B, patients in the Triple group received a higher dose of dexamethasone than those in Double group, in terms of both cumulative dose (median 94.5 mg and 60.0 mg, respectively; P = 0.031) and average dose per day (median 8.9 mg/day and 6.0 mg/day; P < 0.001). The duration of dexamethasone treatment did not differ statistically between the two groups. Patients in the Triple group received their first

Table 2
Treatment and outcomes of the cohort patients.

Variables	Double immune modulator (n = 52)	Triple immune modulator (n = 50)	*P* value
Dexamethasone			
Dexamethasone Tx	52 (100.0)	50 (100.0)	1.000
Duration of Tx	10.0 (8.3–20.8)	10.0 (7.0–17.3)	0.184
Cumulative dose of dexamethasone	60.0 (48.0–101.6)	94.5 (51.5–170.3)	0.031
Average dose of dexamethasone per day	6.0 (5.4–6.0)	8.9 (7.4–11.4)	<0.001
Tocilizumab			
Tocilizumab Tx	52 (100.0)	50 (100.0)	1.000
ICU admission to the 1st dose, days	1.0 (0.3–1.0)	0.0 (0.0–0.0)	<0.001
Second dose Tx	0 (0.0)	12 (24.0)	<0.001
ICU admission to the 2nd dose, days	NA	3.1 ± 1.2	NA
Baricitinib			
Baricitinib Tx	0 (0.0)	50 (100.0)	NA
ICU admission to baricitinib Tx, days	NA	0.0 (0.0–0.0)	NA
Double dose Tx	0 (0.0)	27 (54.0)	NA
ICU admission to dose increase, days	NA	2.0 (2.0–4.0)	NA
Other treatment modalities			
Regdanvimab, prior to ICU admission	0 (0.0)	1 (2.0)	0.305
Remdesivir	51 (98.1)	50 (100.0)	0.324
Antibiotics	20 (38.5)	26 (52.0)	0.232
Clinical outcomes			
Recovery within 30 days (WHO-CPS ≤ 4)	38 (73.1)	49 (98.0)	<0.001
Slope of FiO_2 until HD 15	−1.9 ± 0.1	−3.1 ± 0.1	<0.001
Duration of hospital stay	15.0 (11.0–27.5)	13.8 ± 9.2	0.001
Endotracheal intubation (WHO-CPS 7 or 8)	20 (38.5)	1 (2.0)	<0.001
ECMO support (WHO-CPS 9)	3 (5.8)	1 (2.0)	0.327
In-hospital mortality (WHO-CPS 10)	3 (5.8)	1 (2.0)	0.327
Infectious complications			
Bacterial infection, culture-proven	10 (19.2)	1 (2.0)	0.008
Pneumonia	10 (19.2)	0 (0.0)	0.001
Urinary tract infection	0 (0.0)	1 (2.0)	0.305
COVID-19 associated pulmonary aspergillosis	2 (3.8)	1 (2.0)	0.581

Data are expressed as the number (%) of patients, mean ± SD, or median (IQR) values unless indicated otherwise.
Abbreviations: Tx, treatment; ICU, intensive care unit; NA, not applicable; FiO_2, fraction of inspired oxygen; HD, hospital day; WHO-CPS, World Health Organization Clinical Progression Scale; ECMO, extracorporeal membrane oxygenation.

dose of TOC earlier than those in the Double group (median 0.0 days from ICU admission and 1.0 days; $P < 0.001$). Twenty-four percent of patients in the Triple group received a second dose of TOC, with a median interval of 3.1 days from ICU admission.

Significantly more patients in the Triple group (98.0%) than the Double group (73.1%; $P < 0.001$) experienced clinical recovery within 30 days. This difference was also found using the Kaplan Meier method with the log rank test ($P < 0.001$; Fig. 1A). In all patients, the oxygen requirement decreased over to time (P for time effect <0.001), and there was a significant group-by-time interaction between the two groups over time ($P < 0.001$; Fig. 1B). The observed decrease in oxygen requirement with drug usage also indicates that the patient's clinical improvement is likely attributable to a positive response to the medication. The decreasing slope of FiO_2 until HD 15 was steeper in the Triple group (−3.1 ± 0.1) than the Double group (−1.9 ± 0.1; $P < 0.001$). Significantly fewer patients in the Triple group (2.0%) than the Double group (38.5%; $P < 0.001$) received endotracheal intubation. Duration of hospital stay was significantly shorter in the Triple group, and significantly fewer patients in the Triple group (2.0%) than the Double group (19.2%; $P = 0.008$) experienced culture-proven bacterial infections. The incidence of CAPA did not differ statistically between the groups. Next, we analyzed the serum levels of various inflammatory cytokines, encompassing pro-inflammatory cytokines such as IL-1RA (an inhibitor of IL-1β), IL-6, and TNF-α, chemokines such as CCL3, CCL4, and CCL5, and effector cytokines primarily secreted by T cells, including IFN-γ, IL-4, and IL-10, following the administration of treatment with another COVID-19 cohort. The levels of the majority of the inflammatory cytokines exhibited a gradual decrease after immunosuppressant treatment, with a more pronounced reduction observed in the Double or Triple group (Supplementary Fig. 3).

To identify potential confounding factors for the probability of 30-day recovery, we conducted a univariable analysis for each variable (Supplementary Table 1). FiO_2 at ICU admission (HR 0.966, 95% CI 0.954–0.979; $P < 0.001$), albumin level (HR 2.046, 95% CI 1.468–2.851; $P < 0.001$), underlying pulmonary disease (HR 2.579, 95% CI 1.113–5.976; $P = 0.027$), underling solid cancer (HR 3.332, 95% CI 1.018–10.905; $P = 0.047$), and triple immune modulator therapy (HR 2.332, 95% CI 1.506–3.609; $P < 0.001$) were all statistically significant in the univariable analysis. In the multivariable analysis considering all these variables, FiO_2 at ICU admission (HR 0.963, 95% CI 0.949–0.9789; $P < 0.001$) and triple immune modulator therapy (HR 2.772, 95% CI 1.251–6.147; $P = 0.012$) remained statistically significant factors in 30-day recovery (Table 3).

3.3. Transcriptome changes in blood immune cells before and after GC treatment

To investigate the underlying immunologic mechanism of better clinical outcomes by triple immune modulator therapy, we analyzed PBMCs serially obtained from patients with severe COVID-19 ($n = 24$) before and after they received Single ($n = 6$), Double ($n = 6$), or Triple ($n = 12$) immune modulator therapy. We subjected the 89,382 filtered PBMCs to the uniform manifold approximation and projection (UMAP) algorithm (Fig. 2A) (35), and annotated 13 cell types based on the expression of canonical marker genes (Fig. 2B, Supplementary Fig. 4A).

First, we focused on transcriptomic changes in whole PBMCs before and after GC treatment to evaluate the cellular response to GC treatment. DEGs between the pre-GC and post-GC day 1 PBMCs showed that interferon (IFN)-stimulated genes (ISGs) were notably downregulated by GC (Fig. 2C, left) and these downregulated gene were significantly enriched with steroid responsive gene set (Supplementary Fig. 4B), so we defined those downregulated DEGs as the '*steroid responsive gene set*'. DEGs between pre-steroid and post-steroid day 3 contained similarly downregulated ISGs (Fig. 2C, right). In the steroid responsive gene set, protein-protein interactions among the 50 most downregulated genes were evaluated using a STRING analysis (Fig. 2D) (36). The clustering result of those top 50 DEGs shows that a group of ISGs with dense interactions (cluster 2) and a group with cytotoxic molecules and activation markers (cluster 1; *CD69, GZMB*, and *NKG7*) were downregulated by GC. In GO analysis, the steroid responsive gene set was significantly enriched in both type I IFN and type II IFN response-related pathways (Fig. 2E). We performed a GSEA using a ligand-stimulated gene set (LINCS L1000) to compare cytokine signatures enrichment. Type I IFN - and type II IFN-stimulated genes were strongly associated with both the steroid responsive gene set and the severe COVID-19 gene set in PBMCs from patients with severe COVID-19 (Fig. 2F) (34). Intriguingly, IL-6-, TNF-α-, and IL-1-stimulated genes were enriched in the severe COVID-19 gene set, in additional to the type I and II IFN signatures, but they

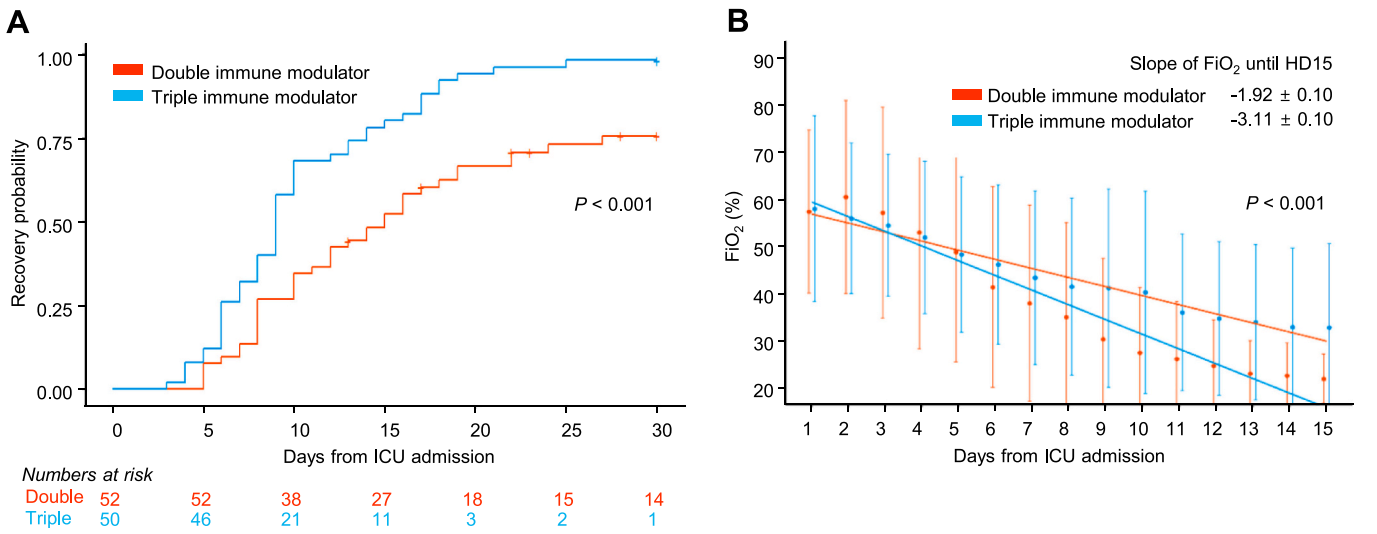

Fig. 1. Clinical outcomes of the Double and Triple immune modulator groups.
A. Graph showing 30-day recovery probability of each treatment group, as calculated by the Kaplan Meier method. B. Graph showing changes in oxygen requirements by hospital day in each treatment group using a linear mixed model.
Abbreviations: FiO_2, fraction of inspired oxygen; HD, hospital day; ICU, intensive care unit.

Table 3
Univariable and adjusted analyses for 30-day recovery.

Variables	Univariable analysis		Adjusted analysis	
	HR (95% CI)	*P* value	HR (95% CI)	*P* value
FiO_2 at ICU admission	0.966 (0.954–0.979)	<0.001	0.963 (0.949–0.978)	<0.001
Albumin level	2.046 (1.468–2.851)	<0.001	0.829 (0.439–1.563)	0.562
Underlying pulmonary disease	2.579 (1.113–5.976)	0.027	2.094 (0.802–5.466)	0.131
Underlying solid cancer	3.332 (1.018–10.905)	0.047	1.819 (0.475–6.960)	0.382
Triple immune modulator treatment	**2.332 (1.506–3.609)**	**<0.001**	**2.772 (1.251–6.147)**	**0.012**

Univariable analyses for 30-day recovery were conducted for each variable, and statistically significant variables were included in the adjusted analysis.
Abbreviations: HR, hazard ratio; CI, confidence interval; FiO_2, fraction of inspired oxygen; ICU, intensive care unit.

were not enriched in the steroid responsive gene set. A GSEA based on the ranked steroid responsive gene set also demonstrated significant associations with the severe COVID-19 gene set and IFN-α-responsive gene set, but not with the IL-6-responsive gene set (Fig. 2G). Collectively, we found that the downregulating effects of GC were mostly associated with IFN responses, which play a critical part in the pathogenesis of severe COVID-19.

3.4. Additive down-modulation of aberrant cytokine responses by the Double and Triple immune modulating strategies

Next, we analyzed scRNA-seq data of PBMCs longitudinally collected from patients with severe COVID-19 in the Single, Double, and Triple groups to evaluate the cellular response to multiple immune modulator treatments added to GC treatment. The gene set module scores for the inflammatory cytokine signaling pathway and severe COVID-19 gene set were additionally downregulated in the post treatment status of Double and Triple groups (Fig. 3A). To identify specific responsive gene sets for each immunomodulation strategy, we produced Venn diagrams to show the similarities and differences among genes significantly downregulated in three treatment groups (Fig. 3B). Genes commonly downregulated among the three treatment groups ($n = 30$) had significantly enriched IFN-γ- and IFN-α-stimulated transcriptome signatures (Fig. 3C). Most of the GC-responsive genes ($n = 247$) from the Single group were GC-specifically downregulated genes ($n = 188$) with a highly enriched with IFN-α-stimulated signature. The genes specifically downregulated in the Double group ($n = 112$) prominently affected the IL-6-associated transcriptome signature, which reflects the use of TOC, as expected. Interestingly, the genes specifically downregulated in the Triple group ($n = 47$) were enriched to IFN-γ-, IFN-α-, TNF-, and IL-6-stimulated signatures, which suggests that adding BAR produced additional downregulation of type I and II IFN signatures beyond that provided by GC- and TOC- treatment. The protein–protein interaction analysis using STRING showed that genes commonly downregulated in all three treatment groups ($n = 30$) contained a cluster of IFN-responsive genes with dense interactions (*STAT1*, *IRF7*, *MX1*, *IFITM1*, and *EPSTI1*) known to be related to unphosphorylated IFN-stimulated gene factor 3 (ISGF3), which is associated with delayed and pathologic IFN-stimulated responses (Fig. 3D, left) (37).

For the specific pathway analysis, MSigDB Hallmark including the gene sets of IFN-γ response, IFN-α response, TNF-α signaling via NF-κB, and IL-6/JAK/STAT3 signaling were used (Supplementary Fig. 5A). For the IFN responses, the Triple group were more enriched than GC-specific or the Double group specific ones, indicating that JAK inhibitor had additional down-regulating effect on IFN pathways. However, for the TNF-α signaling via NF-κB pathway, GC-specific and the Double specific downregulated genes were more enriched than the Triple group. As expected, the Double group specific down-regulated genes mainly reflecting the effect of TOC had strongest enrichment on IL-6/JAK/STAT3 signaling pathways. Moreover, we additionally evaluated transcription factor (TF) analysis. Triple group specific down-regulated genes were highly enriched to the RFX-associated pathways mainly associated with significant downregulation of HLA molecules (Supplementary Fig. 5B). In addition, IRF1 and STAT3 pathways were specifically downregulated by the Triple regimen. Therefore, the BAR and TOC contributed differentially to down-regulate inflammation in COVID-19 patients who received the Triple regimen.

Moreover, the genes specifically downregulated in the Triple group ($n = 47$) also had a distinct cluster of ISGF3, including *OAS1*, and *OASL* (Fig. 3D, right). Based on the recent report that heterozygous OAS1 gain-of-function (GOF) variants cause autoinflammation (38), we tested similarities between gene sets from OAS1 GOF patients with aberrant

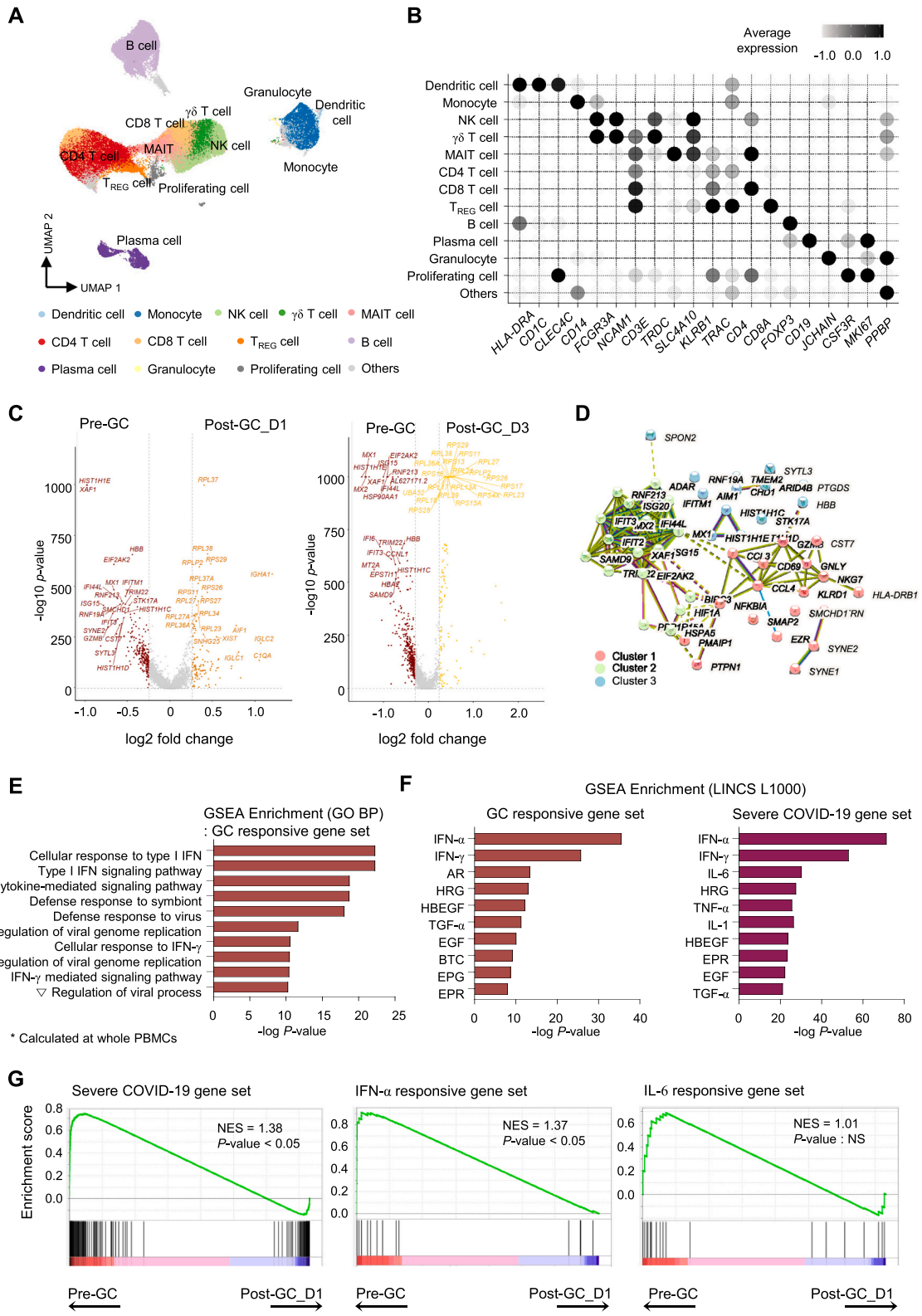

Fig. 2. scRNA-seq analysis of PBMCs from patients with severe COVID-19 treated with GC and biologics.
A. UMAP plot of 89,382 PBMCs from patients with severe COVID-19 sampled pre- and post-medication, colored to show the annotated cell types (COVID-19 patients, $n = 24$). B. Dot plot showing the average marker gene expression in each cluster. C. Volcano plot showing differentially expressed genes between pre- and post-GC treatment at day 1 and day 3. D. Network plot of protein–protein interactions among the top 50 steroid-responsive genes, evaluated using a STRING analysis. E–F. Bar plots showing the -log *P*-value from a GSEA of steroid-responsive genes and the immune-related GO.BP gene sets (E) and the -log *P*-value from a GSEA of steroid-responsive genes and the severe COVID-19 gene set (GSE149689) with the LINC L1000 gene sets (F). G. Plots showing a GSEA of the steroid-responsive gene sets with the severe COVID-19 gene set and gene sets related to the inflammatory cytokine signaling pathways.
Abbreviations: COVID-19, coronavirus disease 2019; GC, glucocorticoid; GO.BP, Gene Ontology, Biological Process; GSEA, gene set enrichment analysis; PBMC, peripheral blood mononuclear cell; scRNA-seq, single-cell RNA sequencing; UMAP, uniform manifold approximation and projection.

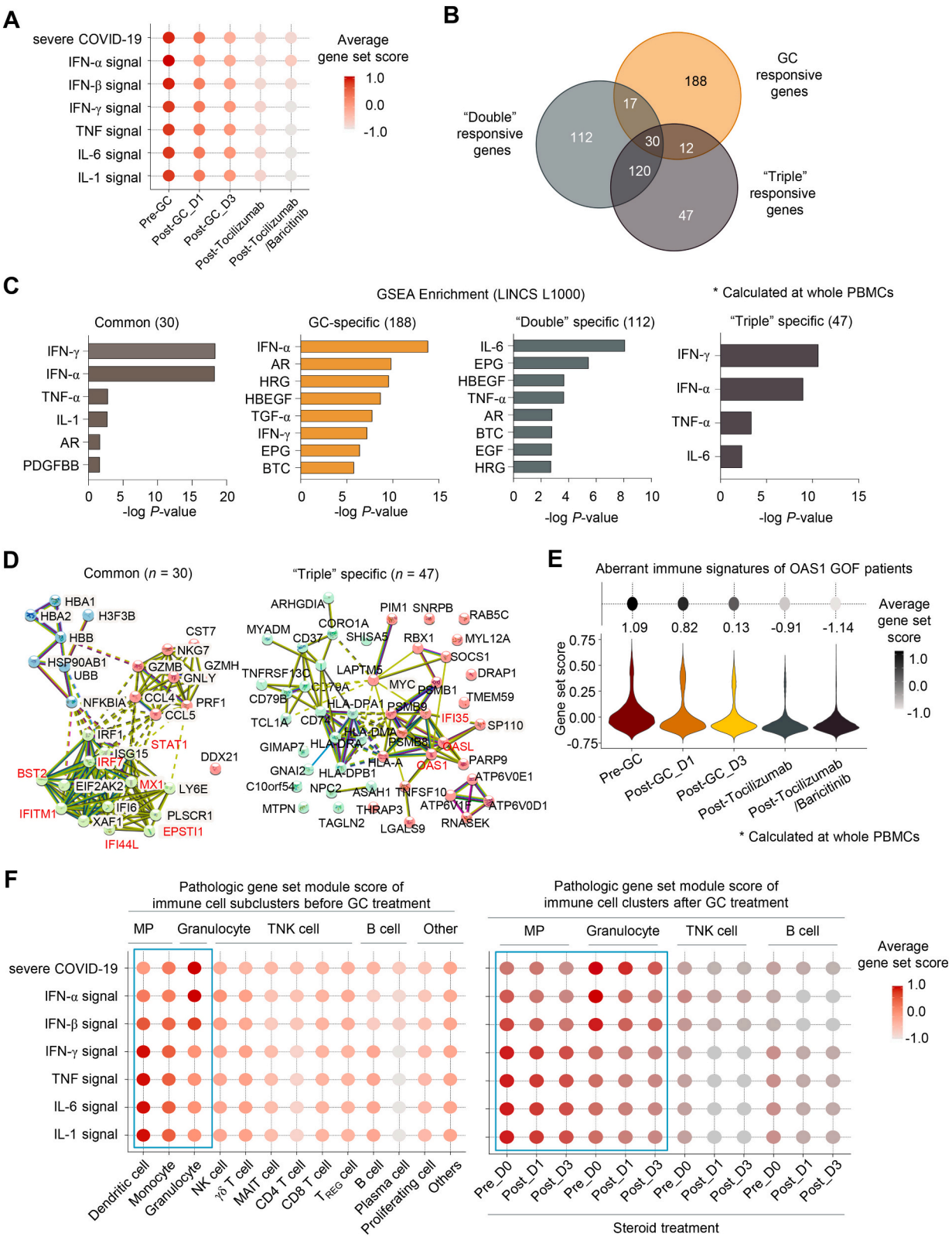

Fig. 3. Additive down-modulation of aberrant IFN responses with the double and triple immune modulating strategies.
A. Dot plot showing the average gene set module score for gene sets related to severe COVID-19 and the inflammatory cytokine signaling pathways according to immunosuppressive treatment. B. Venn diagram of genes responsive to each medication, as calculated by post-medication to pre-medication DEGs. C. Bar plot showing the -log *P*-value from a GSEA of genes responsive to each medication with the LINC L1000 gene sets. D. Network plot of protein–protein interactions among the "Common" and "Triple specific" genes, evaluated using a STRING analysis. E. Plots showing the average gene set module score associated with the aberrant immune signature of OAS1 GOF patients according to immunosuppressive treatment. F. Dot plot showing the average gene set module score of gene sets related to severe COVID-19 and the inflammatory cytokine signaling pathways according to immune subset and steroid treatment.
Abbreviations: DEG, differentially expressed gene; GOF, gain-of-function; GSEA, gene set enrichment analysis.

immune signatures and our gene sets from the different treatment status. The gene set score of aberrant immune signatures from OAS1 GOF patients was significantly downregulated by GC and TOC and even more highly downregulated by BAR (Fig. 3E). In summary, downregulation of the OAS1-associated IFN-responsive signature in the Triple group could be an important mechanism behind the additional clinical efficacy of JAK inhibitors against aberrant cytokine signals.

We next tried to discover whether a specific subpopulation had more cytokine-stimulated and severe COVID-19-associated features by examining transcriptomic changes in the overall blood immune cell populations (Fig. 3F, left). We found that the myelophagocyte (MP) and neutrophil subclusters had higher module scores before GC treatment than others. After GC treatment, those elevated module scores were not evidently downregulated in the MP or neutrophil subclusters (Fig. 3F, right). We further analyzed the cellular response of pathologic MP and neutrophil subclusters upon treatment with multiple immune modulators.

3.5. Triple immune modulator treatment regulates pathologic monocyte differentiation

Among the 7918 MP cells, we identified six subpopulations based on marker gene expression (Fig. 4A, Supplementary Fig. 6A, and Supplementary Table 2). We focused on monocytes and identified three classical CD14 monocyte subpopulations and two intermediate or nonclassical CD16 monocyte subpopulations (Supplementary Fig. 6B). Next, we analyzed the differential marker gene expression representing the differentiation and functional status of the monocytes in each subpopulation. The CD14 monocyte_1 subpopulation was characterized by early activation markers such as *S100A8* and *S100A9*, and the expression level of *S100A8* and *S100A9* gradually decreased across the other monocyte subpopulations (Fig. 4B). The CD16 monocyte_2 subpopulation exhibited high expression of genes related to differentiated monocytes, including the *CD74* and HLA genes, and interferon responsiveness, including *RGS2* and *APOBEC3A*. When we compared the proportions of monocyte subpopulations in patients exposed to each immune modulator treatment strategy, we found that the CD16 monocyte_2 subpopulation tended to decrease in all treatment groups, especially the post-triple group (Fig. 4C). Furthermore, the CD16 monocyte_2 subpopulation was most highly enriched in gene sets associated with severe COVID-19 and inflammatory cytokine signals, indicating that the CD16 monocyte_2 subpopulation is pathologic in severe COVID-19 (Fig. 4D).

Next, we delineated the driving force for differentiating of the pathologic CD16 monocyte_2 subpopulation from the early activated classical CD14 monocyte_1 subpopulation. We performed a semi-supervised pseudotime trajectory analysis by ordering the cells using DEGs from each monocyte subpopulation and identified a pseudotime trajectory pathway across monocyte subpopulations (Fig. 4E) (39). We calculated DEGs according to kinetic trends of the pseudotime trajectory pathway and defined three distinctive clusters with modular gene expression changes (Fig. 4F). Cluster 3 contained genes related to monocyte-to-tissue macrophage differentiation such as *MARCO* (40–42), and DEGs of pathologic alveolar macrophages common in macrophage activation syndrome, such as *C1QB, C1QC, KLF2*, and *FABP5* (43). When we performed a GSEA with DEGs from CD16 monocyte_2 and the genes responsive to each immune modulator treatment strategy, we found that only the Triple responsive genes significantly correlated with the DEGs of CD16 monocyte_2 (Fig. 4G). Taken together, these results suggest that adding BAR treatment to GC and TOC regulates the pathologically activated monocyte subpopulation induced by aberrant IFN signals.

3.6. Landscape of cellular immune responses in neutrophils exposed to multiple immune modulators

Next, we analyzed the cellular response of immune cells other than monocyte. First, we focused on the NK and T cell population, and we identified 6 subpoulations, including, NK cell/γδ T cell, Naïve CD4 T cell, Naïve CD8 T cell, Effector/Memory CD4 T cell, Effector/Memory CD8 T cell (including MAIT cell), and T_{REG} cell (Supplementary Fig. 7A and 7B). Pearson correlation coefficient (PCC) analysis revealed less differentiated subpopulations, such as Naïve CD4 T cell, Naïve CD8 T cell, and Effector/Memory CD4 T cell, had more distant gene expression profiles between pre- and post-treatment with GC (Supplementary Fig. 7C and 7D), indicating significant transcriptomic reprogramming in these subpopulations during treatment. Moreover, through Gene Set Enrichment Analysis (GSEA) using GC responsive gene sets for each subpopulation, we identified that the cellular response to type I IFN was primarily regulated by GC treatment (Supplementary Fig. 7E).

Then, we analyzed the cellular responses of neutrophils to immune modulator treatments. Because of difficulties with isolating polymorphonuclear cells and the instability of neutrophils during cryopreservation, we constructed scRNA-seq libraries of whole leukocytes from RBC-lysed, unfrozen, fresh whole blood. We profiled and clustered 60,000 leukocytes from three patients with severe COVID-19 pre- and post-medication. These clusters were assigned to six major immune cell types, including neutrophils, and were characterized by *MA4A3* and *CEBPE* expression (Fig. 5A and B). The neutrophil subcluster was most highly enriched with gene sets related to severe COVID-19 and those severe COVID-19 gene set enrichments decreased after immunomodulator treatment, especially in the post-TOC/BAR treatment group (Fig. 5C). We further analyzed the heterogeneity of the neutrophil subcluster and identified four neutrophil subpopulations (Fig. 5D). When we plotted the UMAP embedding of neutrophils according to immune modulator treatment status, we found that neutrophils from the pre-GC group were mainly clustered in the Neutrophil_1 subpopulation (Fig. 5E). Neutrophils from the post-GC group were mainly clustered in Neutrophil_2 and Neturophil_3 and neutrophils from the post-TOC/BAR group were mainly clustered in Neutrophil_4. When we calculated the gene set module score associated with severe COVID-19, Neutrophil_1 was more highly enriched with gene sets related to severe COVID-19 than the other subpopulations (Fig. 5F). We assumed Neutrophil_1 to be a pathologic neutrophil subpopulation in patients with severe COVID-19, so we characterized it using a GSEA with GO database (Fig. 5G). The Neutrophil_1 subpopulation was enriched with gene sets related to neutrophil activation, such as neutrophil degranulation, neutrophil activation, and the neutrophil-mediated immune response. In summary, we landscaped and delineated the cellular immune response of leukocytes in the presence of multiple immune modulators and identified pathologic monocyte and neutrophil subpopulations that could be regulated by adding BAR to GC and TOC treatment.

4. Discussion

Traditionally, immune modulating treatments, especially GC, failed to improve the clinical outcomes of severe respiratory viral infections (44,45). However, severe COVID-19 presents delayed worsening of pneumonia despite decreasing viral load, suggesting that it has a unique pathophysiology (46–48). In July 2020, the RECOVERY trial reported that dexamethasone treatment conferred a survival benefit in severe COVID-19 (11). However, initial RCTs to evaluate the effects of TOC on COVID-19 failed to show its clinical benefits (49–52). Interestingly, later studies that allowed co-administration of GC and TOC exhibited survival benefits (12,53). In the ACTT-2 trial, adding BAR treatment to remdesivir showed recovery superior to that with remdesivir alone (54), and a later trial that allowed co-administration of GC and BAR found that BAR treatment conferred a survival benefit (13,55). Given the results of those clinical trials and the different target molecules and mechanisms of action of the different immune modulators, combinations of immune modulator treatments seem likely to show synergistic effects against severe COVID-19.

In terms of clinical recovery, decrease in slope of required FiO2, and

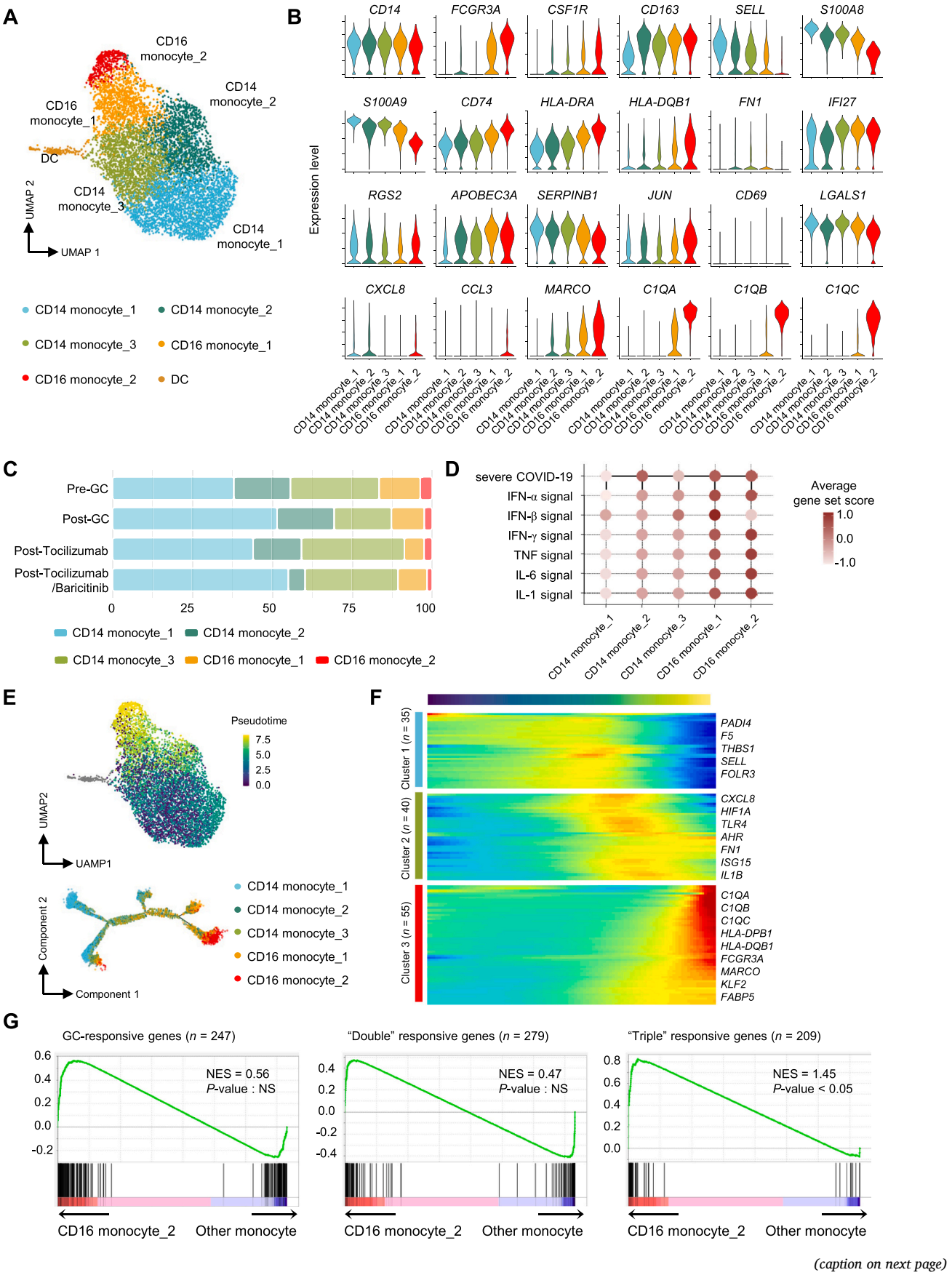

(caption on next page)

Fig. 4. Cellular response of the monocyte population against multiple immune modulator treatments.
A. UMAP plot of 7198 monocyte subpopulations, colored to show cluster information. B. Violin plots showing normalized expression of marker genes in the five monocyte clusters. C. Bar plot showing the proportion of each monocyte subcluster pre-steroid ($n = 5$), post-steroid ($n = 16$), post-double treatment ($n = 3$), and post-triple treatment (n = 3). D. Dot plot showing the average gene set module score of gene sets related to severe COVID-19 and the inflammatory cytokine signaling pathways of the monocyte subclusters. E. Plots showing the pseudotime trajectory of the monocyte subpopulations. F. Heatmap showing the relative expression patterns of representative genes along the pseudotime trajectory. G. Plots showing a GSEA of the pathologic CD16 monocyte_2 subpopulation using gene sets responsive to each medication.
Abbreviations: GSEA, gene set enrichment analysis; UMAP, uniform manifold approximation and projection.

duration of hospitalization, triple immune modulator therapy was more effective than double immune modulator therapy. Contrary to general concerns about combining immune modulator therapies (10), the incidence of infections was lower in the Triple group than in the Double group, probably because patients in the Triple group had shorter hospital stays and a lower rate of mechanical ventilation. Through the single cell transcriptome analysis, we identified a GC responsive gene set that was associated with various immune-suppressive responses, as previously reported. Among them, IFN signals were most affected by GC treatment, and IL-6, TNF, and IL-1 signals, which were also enriched in the severe COVID-19 gene set, were less affected. When we analyzed the cellular immune responses to multiple immune modulators, we found that TOC and BAR treatment additionally regulated the aberrant cytokine response of patients with severe COVID-19, especially in terms of IL-6 and IFN, respectively. Furthermore, we identified pathologic monocyte and neutrophil subpopulations with highly enriched pathologic cytokine signatures. The DEGs of those pathologic subpopulations correlated significantly with the BAR/TOC responsive gene sets, indicating that additional BAR/TOC treatment could regulate these pathologic subpopulations. In summary, we showed that adding BAR and TOC treatment to GC conferred a clinical benefit to patients with severe COVID-19, and we elucidated the detailed cellular immune response of each immune modulator treatment.

In this study, we found that combining immune modulator treatments mainly regulates the aberrant type I and II IFN response. The double-edged features of the IFN response in myeloid cells have been reported since early studies of the immune landscape in COVID-19 (56). In the early stages of viral infection, IFNs play a key role in activating the innate immune system. Type I IFN signaling potentiates inflammatory monocytes to activate other innate immune cells, including NK cells and innate lymphoid cells (57,58). Defective type I IFN responses due to a genetic cause or the presence of autoantibodies against IFN were associated with life-threatening COVID-19 (59,60). On the other hand, IFN can contribute to aberrant activation of innate immune cells and drive pathologic tissue damage. The pro-inflammatory functions of type I IFNs have been reported in a SARS-CoV-2-infected animal model and patients with severe COVID-19 (34,61,62). In particular, it has been suggested that delayed IFN response after initial SARS-CoV-2 infection induces progression to severe disease through crosstalk with hyperinflammatory cytokines such as TNF and IL-1 (34). Therefore, timely and appropriate regulation of an aberrant type I IFN response is required to prevent progression to severe COVID-19.

Therapeutic GCs have been widely used to treat immune-dysregulation disorders, such as post-infectious inflammation and rheumatic disease. Despite the widespread use of GCs, only a small portion of their immunoregulatory mechanisms is understood. A previous study delineating the diversity of cellular targets for GC in an allergic dermatitis model showed that the monocyte-macrophage or neutrophil lineages seem to be essential to the immune regulatory functions of GCs (63). However, few studies have evaluated the cellular response of neutrophils to GC stimulation due to the difficulty of neutrophil isolation. In this study, we landscaped the detailed cellular response of immune cells to GC stimulation, including neutrophils, using fresh, serially collected, whole blood specimens. In that way, we identified the heterogeneity and pathologic subpopulations of monocytes and neutrophils and elucidated the regulatory role of GCs in those pathologic subpopulations. Furthermore, we found that TOC and BAR affect those pathologic subpopulations by regulating specific aberrant cytokine signals, IL-6 and IFN, respectively. Collectively, the results of this study shed light on a tailored immune modulatory treatment that could minimize the adverse effects of excessive GC treatment.

The present study has several limitations. First, our retrospective cohort was limited to 102 patients, which is not sufficient to compare in-hospital mortality. Nevertheless, the baseline characteristics were relatively balanced between the groups, and clinical outcomes clearly favored triple immune modulator treatment. Although the baseline CRP level was higher in the Double group than in the Triple group, the difference was not sufficient to affect 30-day recovery in the survival analysis using Cox proportional hazard model. As the albumin level was lower in the Double group than in the Triple group and was significantly associated with 30-day recovery in the univariable analysis, it was included in the multivariable analysis to adjust potential effect to the clinical outcome. In the multivariable analysis, triple immune modulator treatment was significantly associated with 30-day recovery with the highest HR among the included variables. Second, we excluded patients intubated before or on the day of admission to ensure the homogeneity of the cohort population. Because the risk of secondary respiratory tract infection can increase among patients with an artificial airway (64), combination immune modulator therapies should be considered carefully for intubated patients. The incidence of infections was higher in the Double group (10/52, 19.2%) than in the Triple group (1/50, 2.0%; $P = 0.008$), most of which (72.7%) were ventilator-associated pneumonia, occurred five days after endotracheal intubation on average. A subgroup analysis of the Double group exhibited significant association between bacterial infection and intubation ($P = 0.004$). Only one death was attributable to bacterial infection, and the association between infection and death was not significant. Third, our ex vivo analysis used blood specimens collected at Hospital B between August 2020 and November 2021. During that period, the circulating SARS-CoV-2 strains changed, and the triple immune modulator therapy was used only after the delta-dominated outbreak started. However, we exclusively investigated blood specimens from patients with severe COVID-19 who met the criteria for the retrospective cohort (WHO-CPS 6), and the baseline immunologic profiles did not differ depending on time of enrollment. Despite those limitations, this study suggests that triple immune modulator therapy has benefits for clinical recovery and illustrates the in vitro mechanism by which that therapy controls aberrant hyperinflammation in severe COVID-19.

In conclusion, the use of triple immune modulator therapy in patients with severe COVID-19 was associated with improved 30-day recovery by means of additional regulation of an aberrant, hyperinflammatory immune response. The optimal dose and duration of the therapy need to be validated through clinical trials.

Funding

This work was supported by Samsung Medical Center (grant #no. SMO1210321), the National Research Foundation (NRF) of Korea (NRF-2022R1C1C1012634), the Korean Disease Control and Prevention Agency (#2021-ER1605–00), and the Fundamental Research Program (PNK 9350) of the Korean Institute of Materials Science (KIMS).

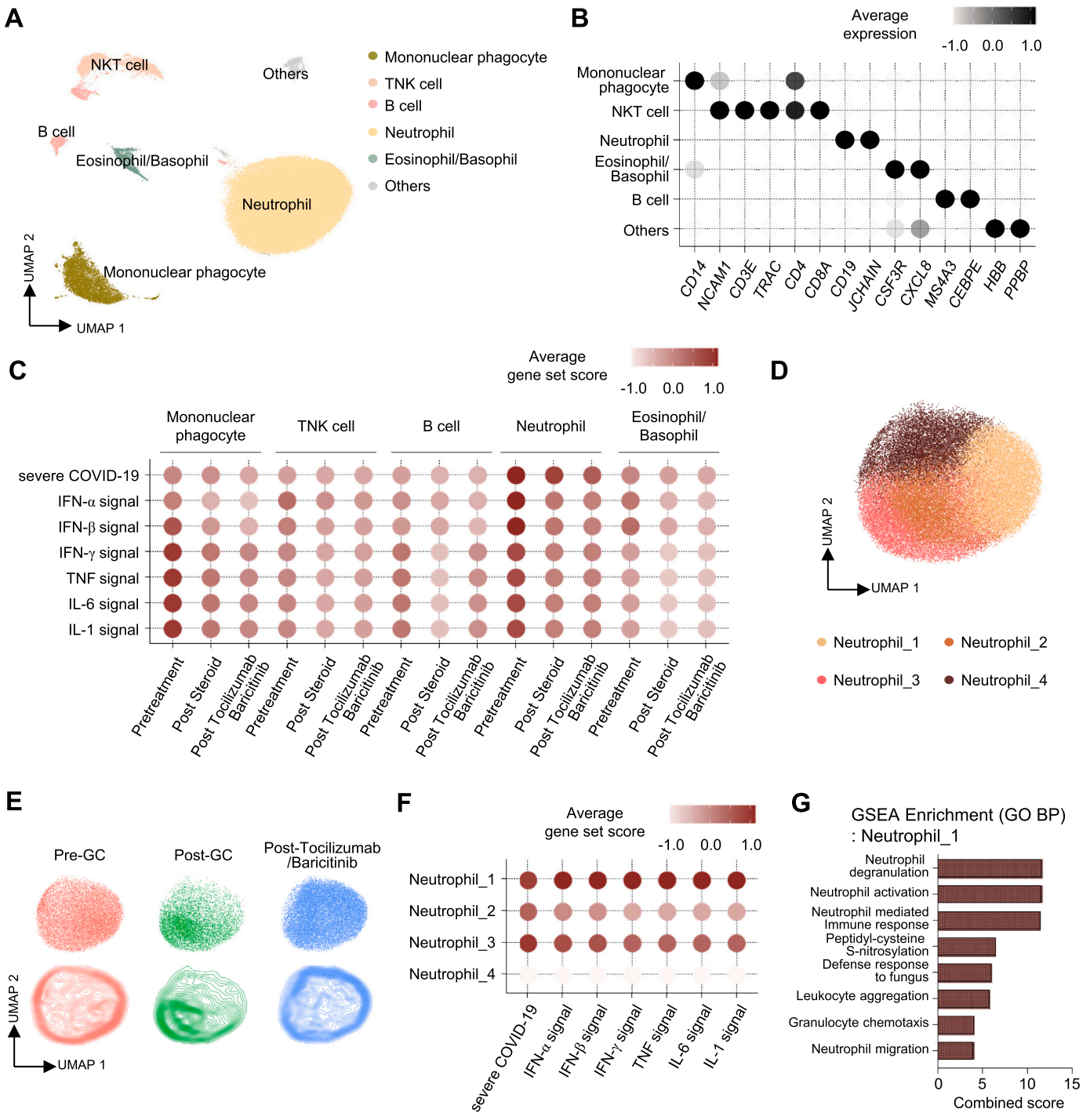

Fig. 5. scRNA-seq analysis of leukocytes from patients with severe COVID-19 treated with multiple immune modulators.
A. UMAP plot of 60,000 leukocytes from patients with severe COVID-19 sampled pre- and post-medication, colored to show the annotated cell types (n = 3). B. Six clusters and their specific marker gene expression levels. C. Dot plot showing the average gene set module scores related to severe COVID-19 and the inflammatory cytokine signaling pathways of immune cell subclusters according to treatment with a steroid, tocilizumab, and baricitinib. D. UMAP plot of 36,601 neutrophils and their subpopulations, colored to show cluster information. E. Dot plots and contour plots showing UMAP embedding of neutrophils, separated according to medication status. F. Dot plot showing the average gene set module score related to severe COVID-19 and the inflammatory cytokine signaling pathways of neutrophil subclusters. G. Bar plot showing the -log *P*-value from a GSEA of DEGs between the pathologic neutrophil_4 subpopulation and the immune related GO.BP gene sets. Abbreviations: scRNA-seq, single-cell RNA sequencing; COVID-19, coronavirus disease 2019; UMAP, uniform manifold approximation and projection; GO.BP, Gene Ontology, Biological Process; GSEA, gene set enrichment analysis; DEG, differentially expressed gene.

Author contributions

Conceptualization and design: J.-H·K, S.-H·K., K.R.P., and J.S.L. Acquisition of data: J.-Y.K., J.-H·K, S.Y.L., S.B., K.H., S.Y.C., C.-I·K, D.R.C, C.R.C., and J.S.L. Analysis and interpretation: J.-Y.K., J.-H·K, S.Y.L., and J.S.L. First manuscript draft: J.-Y.K., J.-H.K, S.Y.L., and J.S.L. Funding acquisition: K.R.P. and J.S.L. Final review and editing: S.-H.K., K.R.P., and J.S.L. All authors critically reviewed and revised the manuscript for intellectual content and approved it before submission.

Declaration of Competing Interest

The authors have no conflicts of interest to disclose.

Data availability

Data will be made available on request.

Acknowledgements

We express our sincerest condolences to the patients and families who have suffered during the COVID-19 outbreak. We greatly appreciate the COVID-19 patients who voluntarily participated in this study by donating blood specimens.

Appendix A. Supplementary data

Supplementary data to this article can be found online at https://doi.org/10.1016/j.clim.2023.109628.

References

[1] R.F. van Vollenhoven, Treatment of rheumatoid arthritis: state of the art 2009, Nat. Rev. Rheumatol. 5 (10) (2009) 531–541.
[2] J.M. Bathon, R.W. Martin, R.M. Fleischmann, J.R. Tesser, M.H. Schiff, E. C. Keystone, et al., A comparison of etanercept and methotrexate in patients with early rheumatoid arthritis, N. Engl. J. Med. 343 (22) (2000) 1586–1593.
[3] R.N. Maini, P.C. Taylor, J. Szechinski, K. Pavelka, J. Bröll, G. Balint, et al., Double-blind randomized controlled clinical trial of the interleukin-6 receptor antagonist, tocilizumab, in European patients with rheumatoid arthritis who had an incomplete response to methotrexate, Arthritis Rheum. 54 (9) (2006) 2817–2829.
[4] M.C. Genovese, J. Kremer, O. Zamani, C. Ludivico, M. Krogulec, L. Xie, et al., Baricitinib in patients with refractory rheumatoid arthritis, N. Engl. J. Med. 374 (13) (2016) 1243–1252.
[5] E. Dufranc, A. Del Bello, J. Belliere, N. Kamar, S. Faguer, IL6-R blocking with tocilizumab in critically ill patients with hemophagocytic syndrome, Crit. Care 24 (1) (2020) 166.
[6] L.A. Henderson, R.Q. Cron, Macrophage activation syndrome and secondary Hemophagocytic Lymphohistiocytosis in childhood inflammatory disorders: diagnosis and management, Paediatr. Drugs. 22 (1) (2020) 29–44.
[7] Y. Zhang, F. Zhou, Z. Wu, Y. Li, C. Li, M. Du, et al., Timing of tocilizumab administration under the guidance of IL-6 in CAR-T therapy for R/R acute lymphoblastic leukemia, Front. Immunol. 13 (2022), 914959.
[8] H. Ewald, H. Raatz, R. Boscacci, H. Furrer, H.C. Bucher, M. Briel, Adjunctive corticosteroids for pneumocystis jiroveci pneumonia in patients with HIV infection, Cochrane Database Syst. Rev. 2015 (4) (2015) Cd006150.
[9] S.L. Hoffman, N.H. Punjabi, S. Kumala, M.A. Moechtar, S.P. Pulungsih, A.R. Rivai, et al., Reduction of mortality in chloramphenicol-treated severe typhoid fever by high-dose dexamethasone, N. Engl. J. Med. 310 (2) (1984) 82–88.
[10] NIH, COVID-19 Treatment Guidelines Panel. Coronavirus Disease 2019 (COVID-19) Treatment Guidelines, National Institutes of Health, 2022. Available at, https://www.covid19treatmentguidelines.nih.gov/. Accessed [May 02, 2022].
[11] P. Horby, W.S. Lim, J.R. Emberson, M. Mafham, J.L. Bell, L. Linsell, et al., Dexamethasone in hospitalized patients with Covid-19, N. Engl. J. Med. 384 (8) (2021) 693–704.
[12] Tocilizumab in patients admitted to hospital with COVID-19 (RECOVERY): a randomised, controlled, open-label, platform trial, Lancet. 397 (10285) (2021) 1637–1645.
[13] V.C. Marconi, A.V. Ramanan, S. de Bono, C.E. Kartman, V. Krishnan, R. Liao, et al., Efficacy and safety of baricitinib for the treatment of hospitalised adults with COVID-19 (COV-BARRIER): a randomised, double-blind, parallel-group, placebo-controlled phase 3 trial, Lancet Respir. Med. 9 (12) (2021) 1407–1418.
[14] F.L. van de Veerdonk, E. Giamarellos-Bourboulis, P. Pickkers, L. Derde, H. Leavis, R. van Crevel, et al., A guide to immunotherapy for COVID-19, Nat. Med. 28 (1) (2022) 39–50.
[15] A. Bhimraj, R.L. Morgan, A.H. Shumaker, V. Lavergne, L. Baden, V.C. Cheng, et al., Infectious diseases society of america guidelines on the treatment and management of patients with COVID-19 (Published by IDSA on 4/11/2020. Last updated, 3/23/2022), Clin. Infect. Dis. (2020) ciaa478.
[16] P. Bost, F. De Sanctis, S. Cane, S. Ugel, K. Donadello, M. Castellucci, et al., Deciphering the state of immune silence in fatal COVID-19 patients, Nat. Commun. 12 (1) (2021) 1428.
[17] C. Musiu, S. Caligola, A. Fiore, A. Lamolinara, C. Frusteri, F.D. Del Pizzo, et al., Fatal cytokine release syndrome by an aberrant FLIP/STAT3 axis, Cell Death Differ. 29 (2) (2022) 420–438.
[18] S. Ramasamy, S. Subbian, Critical determinants of cytokine storm and type I interferon response in COVID-19 pathogenesis, Clin. Microbiol. Rev. 34 (3) (2021).
[19] E. Gavriilidis, C. Antoniadou, A. Chrysanthopoulou, M. Ntinopoulou, A. Smyrlis, I. Fotiadou, et al., Combined administration of inhaled DNase, baricitinib and tocilizumab as rescue treatment in COVID-19 patients with severe respiratory failure, Clin. Immunol. 238 (2022), 109016.
[20] Y. Kai, M. Matsuda, K. Suzuki, T. Kasamatsu, A. Kajita, K. Uno, et al., Tocilizumab and Baricitinib for recovery from acute exacerbation of combined pulmonary fibrosis and emphysema secondary to COVID-19 infection: a case report, Cureus. 14 (3) (2022), e23411.
[21] M. Masiá, S. Padilla, J.A. García, J. García-Abellán, A. Navarro, L. Guillén, et al., Impact of the addition of Baricitinib to standard of care including tocilizumab and corticosteroids on mortality and safety in severe COVID-19, Front. Med. (Lausanne). 8 (2021), 749657.
[22] J. Rosas, F.P. Liaño, M.L. Cantó, J.M.C. Barea, A.R. Beser, J.T.A. Rabasa, et al., Experience with the use of Baricitinib and tocilizumab monotherapy or combined, in patients with interstitial pneumonia secondary to coronavirus COVID19: a real-world study, Reumatol. Clin. (Engl. Ed.). 18 (3) (2022) 150–156.
[23] M.J. Hasan, R. Rabbani, A.M. Anam, S.M.R. Huq, M.M.I. Polash, S.S.T. Nessa, et al., Impact of high dose of baricitinib in severe COVID-19 pneumonia: a prospective cohort study in Bangladesh, BMC Infect. Dis. 21 (1) (2021) 427.
[24] J.Y. Hong, J.-H. Ko, J. Yang, S. Ha, E. Nham, K. Huh, et al., Severity-adjusted dexamethasone dosing and tocilizumab combination for severe COVID-19, Yonsei Med. J. 63 (5) (2022) 430–439.
[25] J.J. Sungchan Yang, Shin Young Park, Seon Hee Ahn, Su Seong-Sun Kim, Bin Park, Boyeong Ryu, Seon-Yeong Lee, Eunjeong Shin, Na-Young Kim, Myeongsu Yoo, Jonggul Lee, Taeyoung Kim, Ae Ri Kang, Donghyok Kwon, COVID-19 outbreak report from January 20, 2020 to January 19, 2022 in the Republic of Korea (https://www.kdca.go.kr/upload_comm/syview/doc.html?fn=164871827898800.pdf&rs=/upload_comm/docu/0034/), Public Health Weekly Report (KDCA). 15 (13) (2022).
[26] E.-J. Joo, J.-H. Ko, S.E. Kim, S.-J. Kang, J.H. Baek, E.Y. Heo, et al., Clinical and Virologic effectiveness of Remdesivir treatment for severe coronavirus disease 2019 (COVID-19) in Korea: a Nationwide multicenter retrospective cohort study, J. Korean Med. Sci. 36 (11) (2021).
[27] A minimal common outcome measure set for COVID-19 clinical research, Lancet Infect. Dis. 20 (8) (2020) e192-e7.
[28] S.-H. Kim, J.Y. Hong, S. Bae, H. Lee, Y.M. Wi, J.-H. Ko, et al., Risk factors for coronavirus disease 2019 (COVID-19)-associated pulmonary aspergillosis in critically ill patients: a Nationwide, multicenter, retrospective cohort study, J. Korean Med. Sci. 37 (18) (2022).
[29] H.M. Kang, M. Subramaniam, S. Targ, M. Nguyen, L. Maliskova, E. McCarthy, et al., Multiplexed droplet single-cell RNA-sequencing using natural genetic variation, Nat. Biotechnol. 36 (1) (2018) 89–94.
[30] L. Haghverdi, A.T.L. Lun, M.D. Morgan, J.C. Marioni, Batch effects in single-cell RNA-sequencing data are corrected by matching mutual nearest neighbors, Nat. Biotechnol. 36 (5) (2018) 421–427.
[31] M.V. Kuleshov, M.R. Jones, A.D. Rouillard, N.F. Fernandez, Q. Duan, Z. Wang, et al., Enrichr: a comprehensive gene set enrichment analysis web server 2016 update, Nucleic Acids Res. 44 (W1) (2016) W90–W97.
[32] The Gene Ontology resource, Enriching a GOld mine, Nucleic Acids Res. 49 (D1) (2021) D325–d34.
[33] M. Niepel, M. Hafner, E.A. Pace, M. Chung, D.H. Chai, L. Zhou, et al., Profiles of basal and stimulated receptor signaling networks predict drug response in breast cancer lines, Sci. Signal. 6 (294) (2013) ra84.
[34] J.S. Lee, S. Park, H.W. Jeong, J.Y. Ahn, S.J. Choi, H. Lee, et al., Immunophenotyping of COVID-19 and influenza highlights the role of type I interferons in development of severe COVID-19, Sci. Immunol. 5 (49) (2020).
[35] A. Butler, P. Hoffman, P. Smibert, E. Papalexi, R. Satija, Integrating single-cell transcriptomic data across different conditions, technologies, and species, Nat. Biotechnol. 36 (5) (2018) 411–420.
[36] D. Szklarczyk, A.L. Gable, K.C. Nastou, D. Lyon, R. Kirsch, S. Pyysalo, et al., The STRING database in 2021: customizable protein-protein networks, and functional characterization of user-uploaded gene/measurement sets, Nucleic Acids Res. 49 (D1) (2021) D605–d12.
[37] H. Cheon, E.G. Holvey-Bates, J.W. Schoggins, S. Forster, P. Hertzog, N. Imanaka, et al., IFNβ-dependent increases in STAT1, STAT2, and IRF9 mediate resistance to viruses and DNA damage, EMBO J. 32 (20) (2013) 2751–2763.
[38] T. Magg, T. Okano, L.M. Koenig, D.F.R. Boehmer, S.L. Schwartz, K. Inoue, et al., Heterozygous OAS1 gain-of-function variants cause an autoinflammatory immunodeficiency, Sci. Immunol. 6 (60) (2021).
[39] C. Trapnell, D. Cacchiarelli, J. Grimsby, P. Pokharel, S. Li, M. Morse, et al., The dynamics and regulators of cell fate decisions are revealed by pseudotemporal ordering of single cells, Nat. Biotechnol. 32 (4) (2014) 381–386.
[40] J.S. Lee, J.Y. Koh, K. Yi, Y.I. Kim, S.J. Park, E.H. Kim, et al., Single-cell transcriptome of bronchoalveolar lavage fluid reveals sequential change of macrophages during SARS-CoV-2 infection in ferrets, Nat. Commun. 12 (1) (2021) 4567.
[41] M. Orecchioni, Y. Ghosheh, A.B. Pramod, K. Ley, Macrophage polarization: different gene signatures in M1(LPS+) vs. classically and M2(LPS-) vs. alternatively activated macrophages, Front. Immunol. 10 (2019) 1084.
[42] J. Xu, A. Flaczyk, L.M. Neal, Z. Fa, A.J. Eastman, A.N. Malachowski, et al., Scavenger receptor MARCO orchestrates early defenses and contributes to fungal containment during Cryptococcal infection, J. Immunol. 198 (9) (2017) 3548–3557.
[43] D.K. Gao, N. Salomonis, M. Henderlight, C. Woods, K. Thakkar, A.A. Grom, et al., IFN-γ is essential for alveolar macrophage-driven pulmonary inflammation in macrophage activation syndrome, JCI Insight. 6 (17) (2021).

[44] Z. Yang, J. Liu, Y. Zhou, X. Zhao, Q. Zhao, J. Liu, The effect of corticosteroid treatment on patients with coronavirus infection: a systematic review and meta-analysis, J. Inf. Secur. 81 (1) (2020) e13–e20.
[45] S.H. Kim, S.B. Hong, S.C. Yun, W.I. Choi, J.J. Ahn, Y.J. Lee, et al., Corticosteroid treatment in critically ill patients with pandemic influenza a/H1N1 2009 infection: analytic strategy using propensity scores, Am. J. Respir. Crit. Care Med. 183 (9) (2011) 1207–1214.
[46] J.Y. Kim, J.H. Ko, Y. Kim, Y.J. Kim, J.M. Kim, Y.S. Chung, et al., Viral load kinetics of SARS-CoV-2 infection in first two patients in Korea, J. Korean Med. Sci. 35 (7) (2020), e86.
[47] D.A. Berlin, R.M. Gulick, F.J. Martinez, Severe Covid-19, N. Engl. J. Med. 383 (25) (2020) 2451–2460.
[48] D.C. Fajgenbaum, C.H. June, Cytokine Storm, N. Engl. J. Med. 383 (23) (2020) 2255–2273.
[49] O. Hermine, X. Mariette, P.L. Tharaux, M. Resche-Rigon, R. Porcher, P. Ravaud, Effect of tocilizumab vs usual Care in Adults Hospitalized with COVID-19 and moderate or severe pneumonia: a randomized clinical trial, JAMA Intern. Med. 181 (1) (2021) 32–40.
[50] C. Salvarani, G. Dolci, M. Massari, D.F. Merlo, S. Cavuto, L. Savoldi, et al., Effect of tocilizumab vs standard care on clinical worsening in patients hospitalized with COVID-19 pneumonia: a randomized clinical trial, JAMA Intern. Med. 181 (1) (2021) 24–31.
[51] J.H. Stone, M.J. Frigault, N.J. Serling-Boyd, A.D. Fernandes, L. Harvey, A. S. Foulkes, et al., Efficacy of tocilizumab in patients hospitalized with Covid-19, N. Engl. J. Med. 383 (24) (2020) 2333–2344.
[52] C. Salama, J. Han, L. Yau, W.G. Reiss, B. Kramer, J.D. Neidhart, et al., Tocilizumab in patients hospitalized with Covid-19 pneumonia, N. Engl. J. Med. 384 (1) (2021) 20–30.
[53] A.C. Gordon, P.R. Mouncey, F. Al-Beidh, K.M. Rowan, A.D. Nichol, Y.M. Arabi, et al., Interleukin-6 receptor antagonists in critically ill patients with Covid-19, N. Engl. J. Med. 384 (16) (2021) 1491–1502.
[54] A.C. Kalil, T.F. Patterson, A.K. Mehta, K.M. Tomashek, C.R. Wolfe, V. Ghazaryan, et al., Baricitinib plus Remdesivir for hospitalized adults with Covid-19, N. Engl. J. Med. 384 (9) (2021) 795–807.
[55] V. Bronte, S. Ugel, E. Tinazzi, A. Vella, F. De Sanctis, S. Cane, et al., Baricitinib restrains the immune dysregulation in patients with severe COVID-19, J. Clin. Invest. 130 (12) (2020) 6409–6416.
[56] C. Lucas, P. Wong, J. Klein, T.B.R. Castro, J. Silva, M. Sundaram, et al., Longitudinal analyses reveal immunological misfiring in severe COVID-19, Nature. 584 (7821) (2020) 463–469.
[57] A.J. Lee, B. Chen, M.V. Chew, N.G. Barra, M.M. Shenouda, T. Nham, et al., Inflammatory monocytes require type I interferon receptor signaling to activate NK cells via IL-18 during a mucosal viral infection, J. Exp. Med. 214 (4) (2017) 1153–1167.
[58] A. Mortha, K. Burrows, Cytokine networks between innate lymphoid cells and myeloid cells, Front. Immunol. 9 (2018) 191.
[59] Q. Zhang, P. Bastard, Z. Liu, J. Le Pen, M. Moncada-Velez, J. Chen, et al., Inborn errors of type I IFN immunity in patients with life-threatening COVID-19, Science. 370 (6515) (2020).
[60] P. Bastard, L.B. Rosen, Q. Zhang, E. Michailidis, H.H. Hoffmann, Y. Zhang, et al., Autoantibodies against type I IFNs in patients with life-threatening COVID-19, Science. 370 (6515) (2020).
[61] B. Israelow, E. Song, T. Mao, P. Lu, A. Meir, F. Liu, et al., Mouse model of SARS-CoV-2 reveals inflammatory role of type I interferon signaling, J. Exp. Med. 217 (12) (2020).
[62] N. Smith, C. Posseme, V. Bondet, J. Sugrue, L. Townsend, B. Charbit, et al., Defective activation and regulation of type I interferon immunity is associated with increasing COVID-19 severity, Nat. Commun. 13 (1) (2022) 7254.
[63] J.P. Tuckermann, A. Kleiman, R. Moriggl, R. Spanbroek, A. Neumann, A. Illing, et al., Macrophages and neutrophils are the targets for immune suppression by glucocorticoids in contact allergy, J. Clin. Invest. 117 (5) (2007) 1381–1390.
[64] A. Mazzariol, A. Benini, I. Unali, R. Nocini, M. Smania, A. Bertoncelli, et al., Dynamics of SARS-CoV2 infection and multi-drug resistant Bacteria superinfection in patients with assisted mechanical ventilation, Front. Cell. Infect. Microbiol. 11 (2021), 683409.